Research on tunable local laser used in ground-to-satellite coherent laser communication

Bin Lu (卢 斌)[1,2], Fang Wei (魏 芳)[1], Zhen Zhang (张 震)[1,2], Dan Xu (徐 丹)[1,2], Zhengqing Pan (潘政清)[1], Dijun Chen (陈迪俊)[1,*], and Haiwen Cai (蔡海文)[1,]**

[1]*Shanghai Key Laboratory of All Solid-State Laser and Applied Techniques, Shanghai Institute of Optics and Fine Mechanics, Chinese Academy of Sciences, Shanghai 201800, China*

[2]*University of Chinese Academy of Science, Beijing 100049, China*

**Corresponding author: djchen@siom.ac.cn; **corresponding author: hwcai@siom.ac.cn*

Received April 22, 2015; accepted July 9, 2015; posted online August 4, 2015

In order to realize homodyne reception and Doppler frequency shift tracking in ground-to-satellite coherent laser communication, a local laser is experimentally demonstrated in this Letter. It is realized based on modulation-sideband injection locking, and has a 10 GHz tuning range, a 1 THz/s tuning rate, a 5 kHz linewidth, and 16 mW of output power. When applied to a Costas loop in a coherent laser communication system, the local laser can achieve ±5 GHz Doppler frequency shift tracking with a 20 MHz/s frequency shift rate, which is sufficient for the ground-to-satellite coherent laser communication.

OCIS codes: 140.3600, 140.3520, 230.2090, 060.1660.

doi: 10.3788/COL201513.091402.

Coherent optical communication has a very high receiving sensitivity, and has become a hot research area in the field of inter-orbit coherent laser communications[1–4]. In a coherent system, a homodyne receiver with a binary phase-shift keying signal modulation can realize the theoretical maximum sensitivity[5]. Homodyne reception requires phase synchronization between the source laser and the narrow-linewidth local laser, which is realized by optical phase-locked loop (OPLL) technology and also requires that the local laser has good frequency tunability[6] to track the Doppler frequency shift. In ground-to-satellite coherent laser communication, it is necessary for the Doppler frequency shift tracking range to be about ±5 GHz, while the maximum Doppler frequency shift rate is nearly 10 MHz/s.

Numerous methods have been presented to meet the requirements mentioned above. Semiconductor lasers have a good frequency tuning property, and can be rapidly tuned by adjusting the temperature or current. However, the linewidth of semiconductor lasers is relatively wide[7]. Fiber lasers with a narrow linewidth can realize frequency tuning by an acousto-optic modulator (AOM)[8,9] or an electro-optic modulator (EOM)[10–12], which can combine the fiber lasers' good properties (robustness and narrow linewidth) with a rapid tuning performance. However, the tuning range is limited by the external radio frequency (RF) signal and the response speed of the modulators, and the output power of the modulated light will be restricted by the modulator's low conversion efficiency. Simultaneous achievement of narrow linewidth operation, fast precision tuning, and high output power is a challenge for a conventional laser source.

In this Letter, a modulation-sideband injection-locking technology is proposed. Through this technology, the good frequency tuning property of semiconductor lasers and narrow linewidth property of fiber lasers can be combined. The master fiber laser is modulated by an EOM to generate many sidebands, and then the modulated light is launched into the semiconductor slave laser. By adjusting the current or temperature of the slave laser, the slave laser will be injection locked at a specific sideband, and the other modes will be suppressed. If the RF signal to the EOM is shifted by $\Delta\omega$, the nth sideband frequency will shift instantly by $n\Delta\omega$; consequently, the frequency tuning rate and range are simultaneously multiplied, overcoming the restriction of the RF signal. Using this technology, the narrow linewidth and stability properties of the main laser can be transferred to the slave laser, and will effectively enhance the output power. Meanwhile, we can easily realize the frequency tuning by altering the RF signal[13–20].

A schematic diagram of the modulation-sideband injection locking is shown in Fig. 1. The master laser is a low-noise fiber laser working in the 1550 nm band. The slave laser is a distributed feedback (DFB) semiconductor laser. The emitting light of the master laser is modulated

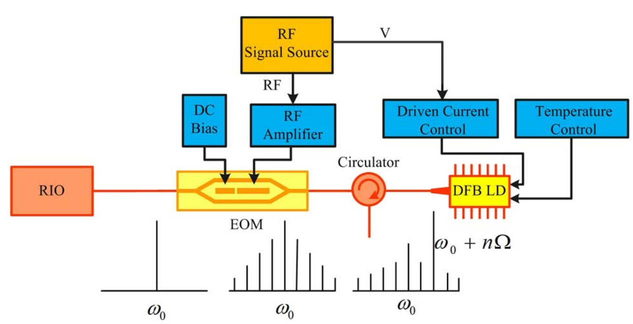

Fig. 1. Schematic diagram of the modulation-sideband injection locking.

through an EOM driven by a RF signal to generate many sidebands. Since the generating procedure of the sidebands is strictly bound to the RF signal and is independent from the cavity reconfiguration, the narrow linewidths of the sidebands are reserved even at a high-frequency tuning rate. We adjust the temperature or current of the slave laser to ensure that a specific sideband is injection locked to the slave laser, and then the frequency tuning can be easily realized by altering the RF signal. There is an injection-locking area (typically hundreds of megahertz for stable injection levels[17]), beyond which the slave laser may lose the locked state. In order to maintain injection locking at the sideband when the frequency is being tuned, synchronous temperature or current compensation is necessary. Considering that the response rate of the temperature compensation is much lower, which will hamper the frequency tuning rate, current compensation is a better choice for rapid frequency tuning.

The operation temperature and current of the DFB slave laser can be set up on the laser driving board. The current driving board not only can set up the bias current, but also has the external current compensation connector, through which an analog voltage can be turned up to linearly adjust the driving current. The measured external current compensation coefficient is about 20 mA/V. Moreover, the frequency tuning and external compensation voltage must be kept synchronous.

The RF signal source is designed to generate both the RF signal and the synchronous compensation voltage. Meanwhile, the RF signal has to keep a low noise in order to not deteriorate the modulated master laser's linewidth. A voltage-controlled oscillator (VCO) is a kind of high-speed voltage-frequency converter. It can rapidly transform a voltage signal into a corresponding RF signal. Meanwhile, the voltage can be processed to act as the synchronous compensation voltage. The parameters of the VCO (Hittite, HMC-C029) we use are shown in Table 1. To guarantee the low-noise property of the RF signal, two ultra-low-noise digital-to-analog converter (DAC) are chosen, and the circuit board is professionally designed and manufactured.

The schematic diagram of the RF signal source is shown in Fig. 2. The output voltage of the two different DAC is added together through an electrical adder to drive the EOM. One is a DAC that is of high precision (20 bit),

Table 1. Parameters of the VCO

Frequency Range	5–10 GHz
Power Output	17–20 dBm
Tune Voltage	0–20 V
Supply Current	195 mA@15 V
Second Harmonic	−15 dBc
SSB Phase Noise	−93 dBc/Hz@100 kHz
	−64 dBc/Hz@10 kHz

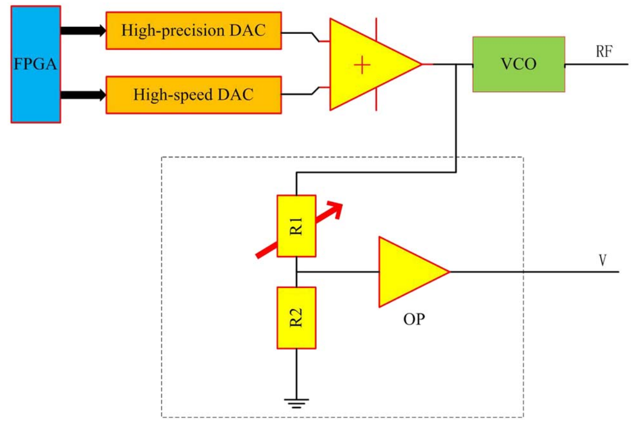

Fig. 2. Schematic diagram of the RF signal source.

has a high output voltage range (0–20 V), and has a low speed (settling time 1 us). The other one is a DAC that is of lower precision (16 bit), has a low output voltage range (0–200 mV), and has a high speed (settling time 400 ps). The voltage output range of the high-precision DAC can drive the VCO to produce a RF signal spanning from 5 to 10 GHz. Driven by the RF signal, the slave laser can realize the large range and lower speed frequency tuning, and can thus fulfill the tracking of the Doppler frequency shift. The high-speed DAC is used to enable the slave laser to conduct a rapid, small-range frequency tuning to make the phase locked instantly in the OPLL system. The output voltage of the adder is processed by an analog circuit, and is attached to the external current compensation connector of the slave laser to fulfill the synchronous current compensation.

The output RF signal of the VCO is measured by a spectrum analyzer (Fig. 3); it indicates that the 3 dB bandwidth is about 5 kHz. Thus, the noise of the RF signal is low enough that it will not deteriorate the linewidth of the modulated master laser, although there are two small sidelobe peaks induced by the noise from the DAC.

The output optical spectra are measured by an optical spectrum analyzer, as shown in Fig. 4. Figure 4(a) is the

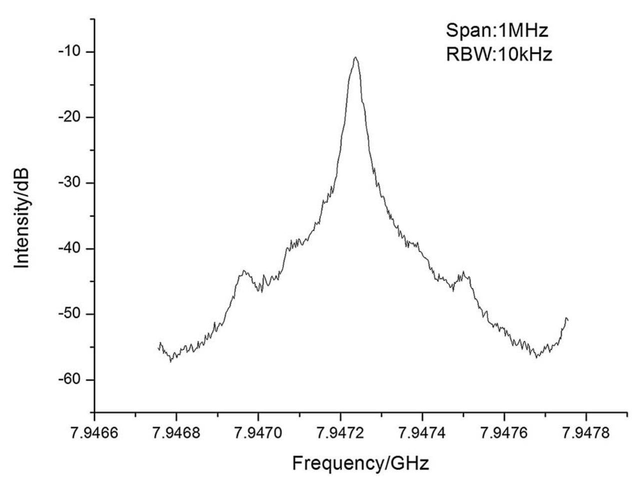

Fig. 3. RF signal spectrum diagram at 7.94796 GHz.

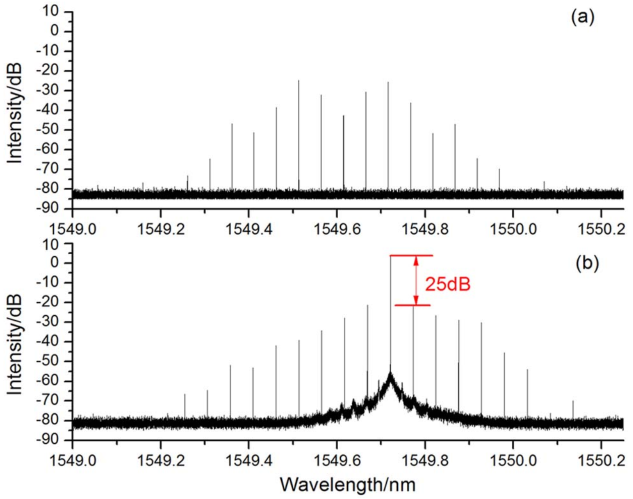

Fig. 4. Spectra of the local laser. (a) Modulated master laser. (b) Injection-locked slave laser.

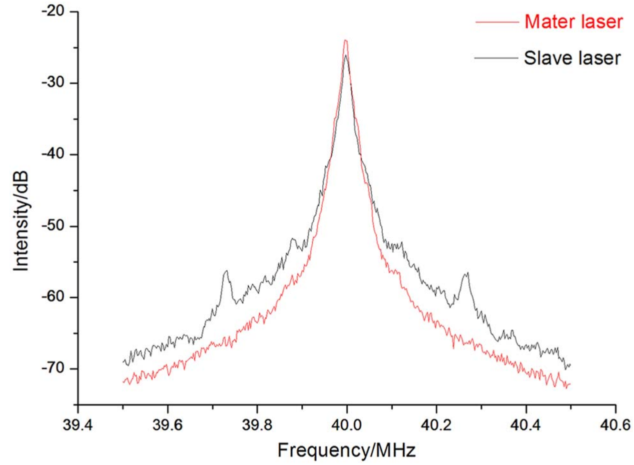

Fig. 5. Linewidths of the master and injection-locked slave lasers.

output spectrum of the EOM modulated by a RF signal of about 6.5 GHz. Figure 4(b) is the output spectrum of the slave laser after being injection locked at the second sideband. It is obvious that the carrier has been effectively suppressed (over 25 dB), and the EOM can generate offset sidebands of up to 45 GHz. The output power is greatly enhanced (more than 30 dB) after injection locking. The output power of the injection-locked slave laser is measured by a power meter. The average power is above 16 mW (almost the same as the output power of the slave laser without injection locking), which is high enough to satisfy the needs in a homodyne reception.

The linewidth of the laser is measured based on a fiber-delayed, self-heterodyne interferometer[21]. The fiber length is about 20 km, and the frequency is about 40 MHz, generated by an AOM. The linewidth of the slave laser without injection locking is nearly 200 kHz. The results after realizing injection locking are presented in Fig. 5: the red line is the linewidth of the master laser, and the black one is the linewidth of the slave laser injection locked at the second sideband of the master laser. It shows that the noise of the locked slave laser is slightly increased compared to the master laser's linewidth. The sidelobe peaks are due to the RF signal induced by the noise of the DAC. The 3 dB linewidth is almost the same as the master laser: <5 kHz. The narrow linewidth property will enable the local laser to be applied to an OPLL system.

In order to demonstrate the large range and rapid frequency tuning ability of the local laser, the high-precision DAC is controlled to drive the VCO to generate a RF signal spanning from 5 to 10 GHz. By adjusting the slave laser to be injection locked at the second sideband of the master laser, the output light-frequency tuning range can be expanded from 5 to 10 GHz. The frequency tuning characteristics are measured by a fiber asymmetric Mach–Zehnder interferometer (see Fig. 6), whose free spectral range is about 220 MHz. Figure 6(a) is the voltage signal of the VCO, and Fig. 6(b) shows the intensity curves of the non-equilibrium Mach–Zehnder interferometer. It can be seen that the frequency-tuning period is approximately 10 ms, and that the number of sinusoidal wave is approximately 49. Then, we can calculate that the frequency tuning range surpasses 10 GHz (220 MHz*49), and that the frequency tuning rate is over 1 THz/s. The frequency tuning performance of the local laser can fulfill the needs of the Doppler frequency shift compensation of a ground-to-satellite coherent laser communication.

Then, the local laser is applied to the Costas OPLL system[22], which is an important part of the coherent optical communication. The signal laser is a kind of fiber DFB laser working in the 1550 nm band. The signal laser can be tuned to around dozens of megahertz through an external voltage, or tuned to around scores of gigahertz by adjusting the signal laser's operating temperature. A frequency difference is set between the signal laser and the local laser. Then, the field programmable gate array controls the local laser to conduct a frequency sweeping. The frequency difference and the beat frequency of the

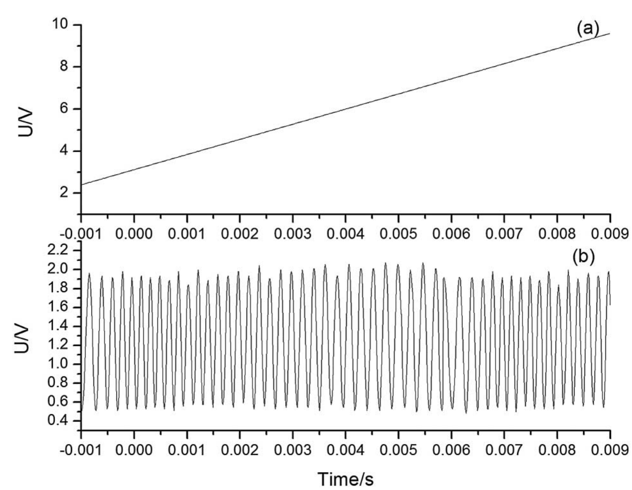

Fig. 6. Intensity curves of the non-equilibrium Mach–Zehnder interferometer for laser frequency modulation.

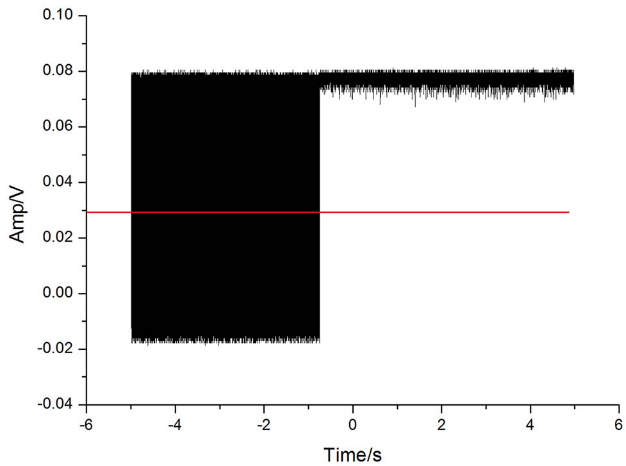

Fig. 7. Capture process.

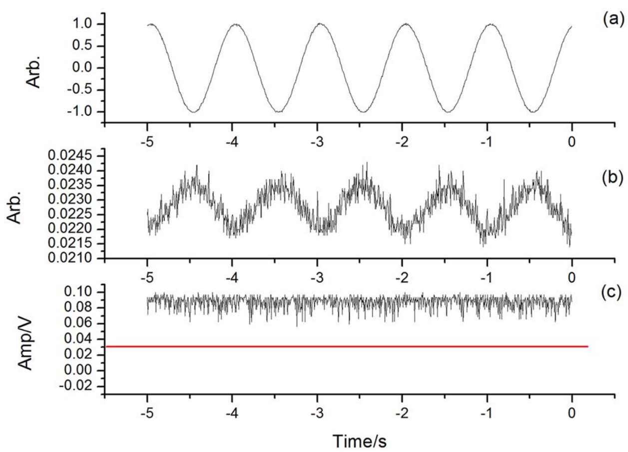

Fig. 8. Doppler frequency shift tracking within 12 MHz.

output sinusoidal wave are gradually reduced, until they are within the capture range of the OPLL. The OPLL will achieve phase locking when the beat frequency is nearly zero. Despite phase locking, some phase noise will still exist. As long as the phase noise does not exceed half of the full-width of the output signal, no error will occur. The capture process is shown in Fig. 7, where the phase noise is within the threshold of red line.

To verify the Doppler frequency shift tracking, the signal laser needs to be frequency tuned to simulate the Doppler frequency shift. The small frequency range tracking process is shown in Fig. 8. The tuning frequency range is approximately 12 MHz, and the simulated Doppler frequency shift rate is nearly 20 MHz/s. Figure 8(a) is the external tuning voltage of the signal laser, Fig. 8(b) is the response of the local laser, and Fig. 8(c) is the phase-locked state. The large-range Doppler frequency shift process is shown in Fig. 9. Due to the frequency tuning limit of the signal laser, the simulated Doppler frequency shift is about 6 GHz, while the tuning rate is nearly 20 MHz/s. Figure 9(a) is the tuning temperature of the signal, Fig. 9(b) is the response of the local laser,

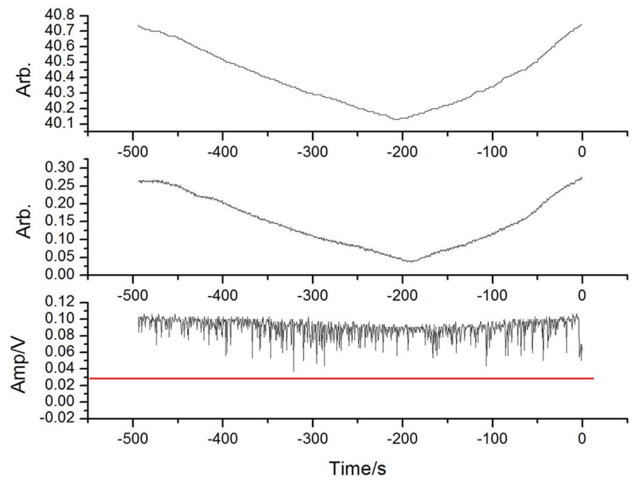

Fig. 9. Doppler frequency shift tracking within 6 GHz.

and Fig. 9(c) is the phase-locked state. While conducting the large frequency range Doppler frequency shift compensation, the phase noise is slightly increased, but is still within the threshold, and is low enough to satisfy the needs of coherent communication.

In conclusion, a tunable local laser used in ground-to-satellite coherent laser communication is presented in this Letter using modulation-sideband injection-locking technology. The local laser has a 10 GHz tuning range, a 1 THz/s tuning rate, a 5 kHz linewidth, and 16 mW of output power. When applied to a Costas OPLL in a coherent laser communication system, the local laser can achieve a 6 GHz Doppler frequency shift tracking range with a 20 MHz/s shift rate. In the future, some efforts will be made to enable the slave laser to be injection locked at a higher sideband of the modulated master laser. Then, the frequency tuning range and tuning rate can be extended.

This work was supported by the National Natural Science Foundation of China (No. 61405218) and the Shanghai Natural Science Foundation (No. 14ZR1445100).

References

1. L. Tan, Y. Yang, J. Ma, and J. Yu, Opt. Express **16**, 13372 (2008).
2. N. Xu, L. Liu, D. Liu, and Y. Zhou, Laser Optoelectron. Prog. **45**, 25 (2008).
3. Y. Zhou, L. Wan, Y. Zhi, Z. Luan, J. Sun, and L. Liu, Acta Opt. Sin. **29**, 3291 (2009).
4. N. Xu, L. Liu, L. Wan, and J. Sun, Acta Opt. Sin. **30**, 347 (2010).
5. T. Okoshi, Lightwave Technol. **2**, 341 (1984).
6. N. Satyan, A. Vasilyev, G. Rakuljic, V. Leyva, and A. Yariv, Opt. Express **17**, 15991 (2009).
7. P. Correc, O. Girard, and I. F. Defaria, IEEE J. Quantum. Electon. **30**, 2485 (1994).
8. B. E. Unks, N. A. Proite, and D. D. Yavuz, Rev. Sci. Instrum. **78**, 083108 (2007).
9. J. Biesheuvel, D. W. E. Noom, E. J. Salumbides, K. T. Sheridan, W. Ubachs, and J. C. J. Koelemeij, Opt. Express **21**, 14008 (2013).

10. A. Kanno, T. Kawanishi, S. Honda, and H. Sotobayashi, in *2010 IEEE Topical Meeting on Microwave Photonics (MWP 2010)* 283 (IEEE, 2010).
11. A. Kanno, S. Honda, R. Yamanaka, H. Sotobayashi, and T. Kawanishi, Opt. Lett. **35**, 4160 (2010).
12. D. Y. Kubo, R. Srinivasan, H. Kiuchi, and C. Ming-Tang, IEEE Trans. Microw Theory Techn. **61**, 3005 (2013).
13. K. Szymaniec, S. Ghezali, L. Cognet, and A. Clairon, Opt. Commun. **144**, 50 (1997).
14. S. E. Park, T. Y. Kwon, and H. S. Lee, IEEE Trans. Inst. Meas. **52**, 277 (2003).
15. H. K. Sung, E. K. Lau, and M. C. Wu, IEEE Photon. Technol. Lett. **19**, 1005 (2007).
16. F. Wei, B. Lu, J. Wang, D. Xu, Z. Pan, D. Chen, H. Cai, and R. Qu, Opt. Express **23**, 4970 (2015).
17. G. J. Schneider, J. A. Murakowski, C. A. Schuetz, S. Y. Shi, and D. W. Prather, Nat. Photon. **7**, 118 (2013).
18. P. Guo and Z. Chen, Chin. Opt. Lett. **11**, 121403 (2013).
19. W. Ji, S. Chen, L. Fu, and Z. Zou, Chin. Opt. Lett. **10**, 080601 (2012).
20. J. Wang, Z. Li, Q. Wu, W. Wang, S. Jia, and J. Yu, Chin. Opt. Lett. **12**, 100607 (2014).
21. L. Richter, H. I. Mandelberg, M. Kruger, and P. McGrath, IEEE J. Quantum Electron. **22**, 2070 (1986).
22. R. Lange and B. Smutny, Proc. SPIE **6877**, 687702 (2008).